Specific electrochemical sensor for cadmium detection: Comparison between monolayer and multilayer functionalization

Gaël Levanen, Awatef Dali, Yann R. Leroux, Teodora Lupoi, Stéphanie Betelu, Karine Michel, Soraya Ababou-Girard, Philippe Hapiot, Ikram Dahech, Cecilia Cristea, et al.

Specific electrochemical sensor for cadmium detection: comparison between monolayer and multilayer functionalization

Gaël Levanen [a,g], Awatef Dali [a, b, g], Yann Leroux [a], Teodora Lupoi [a,c], Stephanie Betelu [d], Karine Michel [d], Soraya Ababou-Girard [e], Philippe Hapiot [a], Ikram Dahech [a], Cecilia Cristea [c], Bogdan Feier [c], Florence Razan [f], Florence Geneste [a]

[a] Univ Rennes, CNRS, ISCR, UMR 6226, F-35000 Rennes, France

[b] Laboratoire des Sciences et Technologies de l'environnement (LSTE), faculté des sciences exactes, département de Chimie, Université des frères Mentouri Constantine 1, Algeria

[c] "Iuliu Hatieganu" University of Medicine and Pharmacy, Faculty of Pharmacy, 4 Pasteur str, 400012 Cluj-Napoca, Romania

[d] BRGM (French Geological Survey), 3 Avenue Claude Guillemin, 45060 Orléans Cedex 2, France

[e] Univ Rennes, CNRS, IPR – UMR 6251, F-35000 Rennes, France

[f] ENS Rennes, SATIE, UMR-CNRS 8029, Campus de Ker Lann 35170 Bruz, France.

[g] Equally contributing

Keywords: electrografting, cadmium detection, electrochemical sensor, diazonium salts, monolayer

Abstract

Selective and sensitive cadmium sensors were prepared by functionalizing glassy carbon electrodes (GCE) using the electrochemical reduction of *p*-benzoic acid diazonium salts according to either a multilayer or a monolayer coating process. Such modified electrodes

were then post-functionalized with 1,2-bis-[o-aminophenylthio]ethane (APTE) or its monoprotected derivative leading to specific Cd^{2+} electrochemical sensors. The step by step preparation of the electrodes as well as the ability of the immobilized receptor to complex Cd^{2+} was investigated by XPS and Raman spectroscopy. The detection and quantification of cadmium was performed in two steps: the preconcentration of Cd^{2+} ions by complexation with immobilized APTE and the analysis by Linear Sweep Stripping Voltammetry (LSSV). More importantly, multilayer *versus* monolayer grafting has a strong influence on the sensor performances. Whereas calibration curves typical of an equilibrium process were obtained for sensors realized with multilayer organic films, sensors with a monolayer organic film led to linear calibration curves, in the same concentration range. Finally, the monolayer sensor gave a lower limit of detection (LOD) and highlighted better selectivity than unmodified electrode.

1. Introduction

Over the last three decades, there is an increasing global concern over the public health impacts ascribed to environmental pollution. Some compounds like Metallic Trace Elements (MTE) have been subject to strict regulation because they are toxic even at trace level. Thus, the exposure to MTE can cause cancer, renal diseases and even death at very high concentration [1].

Among the metallic trace elements widely disseminated in environment by anthropogenic activity [2-4], cadmium is one of the most concerning owning to its very high toxicity [5, 6]. It is worth noting the European drinking water guidelines for cadmium set at 5 µg/L (*i.e.* 4×10^{-8} mol L^{-1}) [7]. Sources of MTE include natural sources, mining, industrial production, untreated sewage sludge and diffuse sources such as metal piping, traffic etc. This pollution could be found in water, soil and could be transferred to the food chain. Before efficient treatments have been achieved, it is essential to develop sensors that are able to control *in situ*

and in semi-continuous manner the concentration of MTE in their most bioavailable form *i.e.* free ions and labile complexes in contaminated samples, the most toxic species forms of MTE [8-10].

In laboratories, the detection of MTE at trace level is performed by Ion Chromatography (IC), Atomic Absorption Spectroscopy (AAS) and Inductive Coupling Plasma coupled with Mass Spectrometry (ICP-MS) or Atomic Emission Spectroscopy (ICP-AES) that allow the detection of several ions in one analysis with concentrations lower than 0.1 µg L^{-1} [11]. Such techniques usually provide the MTE total dissolved content, generally after 0.45 µm filtration and microwave-assisted digestion. For the quantification of the free ions and labile complexes analogous fraction, two filtration methods (ultrafiltration and tangential flow filtration) or centrifugation are required.

For a better insight into the detection and quantitation of free ions and labile complexes on site or *in situ*, electrochemical detection is the most promising. Miniaturized and portable, the electrochemical systems, composed of the electrochemical device, the fluidic system and the associated electrodes, are easily implemented; they benefit from high sensitivity and require short analysis time. The analyses can be performed directly into the raw sample, even for small volumes (~µL) [12]. The direct analysis of raw samples is of great interest. Indeed, accurate and specific techniques should be deployed in order to minimize sample degradation during sampling and handling. The electrochemical detection systems are thus among the most promising decision-making tools regarding the public health impacts ascribed to environmental pollution.

To achieve trace analysis, electroanalytical methods require a preconcentration step before the analysis aiming at accumulating the analyte close to the electrode surface to increase the electrochemical signal. Stripping voltammetry at a static mercury drop electrode is one of the most sensitive analytical method for trace analysis [13]. It allows the simultaneous detection

of metallic ions. Due to the toxicity of mercury, substitute methods have also been developed, consisting in a first step of preconcentration of the analyte onto the electrode surface before the electrochemical analysis, as with anodic stripping voltammetry at a mercury electrode. Among all mercury-substituting electrodes studied [14-17], chemically modified electrodes (CMEs) can trapped cations by different methods such as ion-exchange, complexation, bioaccumulation and hydrophobic interaction. Complexation methods that consist in the introduction of free coordinating sites on the electrode used as specific receptors have been widely used to preconcentrate selectively ions on the electrode surface [18-24]. Advantageously free ions and labile complexes that are able to form complexes with the immobilized receptors will be analyzed. The as prepared electrochemical sensors have led to the detection of ions with high sensitivity and good selectivity mainly due to the specific receptor. Although most reported work focused on the nature of specific receptors to improve the sensitivity and selectivity of the sensors, less attention has been paid on its immobilization process.

Since the covalent modification of electrodes by the reduction of aryldiazonium salts has been proposed [25, 26], this efficient and easy-to-implement method has been widely used for many applications including the preparation of electrochemical sensors [27-32]. The mechanism of electrografting involves the formation of aryl radicals giving rise to stable chemical bounds with the electrode surface such as carbon-carbon bounds [31, 33]. By this way, a stable immobilization of specific receptors can be achieved, promoting a good repeatability and a long-term operation of the sensor. Furthermore, the method could be applied to modify many conducting surfaces including metallic electrodes such as gold, platinum and carbon surfaces such as glassy carbon, carbon nanotubes, and graphene [27]. However, the high reactivity of aryl radical intermediates results in the attack of the already grafted phenyl groups, leading to organic multilayers by carbon-carbon and azo bounds

formation. Compared for example with the well-organized functionalization by alkanethiols, the difficulty to control the reaction appears as an obstacle to the development of sensitive electrochemical sensors. Thus, unexpected complexing capabilities for copper ions have been reported for electrodes functionalized by reduction of 4-methoxybenzene diazonium salts [34]. It was attributed to the presence of methoxy and/or azo groups present inside the multilayer film. The low conductive multilayer can also act as a barrier to electron transfer [35, 36]. A good compromise has to be found since the amount of immobilized species increases with the film thickness whereas the electron transfer kinetic decreases [37]. Interestingly, several original approaches have been reported to better control the electrografting process, leading to the formation of a thin film close to a monolayer [38-44]. Such well-controlled modification processes led to fast reading and low barrier charge transfer [38, 45]. Although a monolayer functionalization promoting electron exchange is expected to be useful for electrochemical sensing, to our knowledge, its real effect on sensors performance has not yet been deeply investigated.

In the course of our research on the preparation of a selective and sensitive electrochemical sensor for the detection of Metallic Trace Elements, we investigated the effect of the electrografting process on the sensor performances. Carbon electrodes were functionalized by reduction of aryldiazonium salts to introduce COOH ending groups in two different ways. The first one consisted in the reduction of 4-carboxybenzenediazonium salts, leading to a multilayer film and the second one involved a protection-deprotection strategy resulting in a monolayer functionalization of the electrode surface [46]. 1,2-bis-[o-aminophenylthio]ethane (APTE) used as Cd^{2+} specific receptor [47] was then immobilized by an amide for a selective preconcentration of Cd^{2+} ions on the electrode surface. The performance of the two sensors in terms of limit of detection, sensitivity, reproducibility and selectivity clearly highlighted the advantage of the monolayer functionalization.

2. Experimental

2.1 Reagents and materials

Lead(II) nitrate, copper(II) nitrate hemipentahydrate, nickel(II) nitrate hexahydrate, zinc(II) nitrate hexahydrate, manganese (II) nitrate terahydrate, chrome(III) nitrate nonahydrate, iron(III) nitrate monohydrate, thionyl chloride, triethylamine and lithium perchlorate 99% were purchased from Acros, cadmium(II) nitrate tetrahydrate from Carlo Erba and mercury(II) chloride, cobalt(II) nitrate hexahydrate from Aldrich. The synthesis of the diazonium salt of 9-*H*-Fluoren-9-ylmethyl 4-Aminobenzoate (N_2^+-Ar-COO-Fm) was performed as reported previously [46]. All solutions were prepared with ultrapure water (18.2 MΩ, Millipore Simplicity). All glassware were rinsed with a 10% HNO_3 solution followed by ultrapure water before use to avoid metal contamination.

2.2 Synthesis of the receptors

1,2-bis-[o-aminophenylthio]ethane (APTE) was synthesized as previously reported [47].

tert-butyl (2-((2-((2-aminophenyl)thio)ethyl)thio)phenyl)carbamate (Boc-APTE). 0.32 g (1.1 mmol) APTE were dissolved in 15 mL of dioxan/H_2O (2:1). After addition of 0.25 g (1.1 mmol) of Di-*tert*-butyl dicarbonate in 15 mL of dioxan/H_2O (2:1), 0.3 mL (2.1 mmol) triethylamine were added dropwise. The mixture was stirred overnight. 0.1 mol L^{-1} HCl solution was added at 0°C until neutral pH. After extraction with 50 mL ethyl acetate, the solution was dried over $MgSO_4$ and concentrated under vacuum. The compound was purified by flash chromatography on silica with dichloromethane/petroleum ether (60:40) eluent. Yield 39%

^{1}H NMR (300 MHz, D_2O), δ: 8.17 (d, J = 6 Hz, 1 H); 7.82 (s, 1 H); 7.44 (dd, J = 6, 1 Hz, 1H); 7.36-7.26 (m, 2H); 7.15 (dt, J = 6, 1 Hz, 1H); 6.96 (dt, J = 6, 1 Hz, 1H); 6.74 (dd, J = 6, 1 Hz, 1H); 6.69 (dt, J = 6, 1 Hz, 1H); 3.92 (s, 2H); 2.91-2.83 (m, 4H); 1.56 (s, 9H).

2.3 Preparation of the modified electrodes

Glassy carbon electrodes were functionalized by reduction of diazonium salts following a previously reported protocol [46] for the monolayer (Mono@GC) and as follows for the multilayer process (Multi@GC):

A solution of 4-amino-benzoic acid (50 mmol L^{-1}) in 0.5 mol L^{-1} H_2SO_4 was cooled to 0°C. After argon deaeration, 3 eq. $NaNO_2$ were added. After 20 min the electrografting process was carried out by cyclic voltammetry with 5 cycles from 0 to -0.6 V/SCE (0.05 V s^{-1}). The electrodes were then rinsed with ultrapure water and dipped in two bathes of ultrapure water.

The Mono@GC and Multi@GC electrodes were then dipped in a solution of 10 mL anhydrous dichloromethane with 1 mL of thionyl chloride. After 1h, the solution was removed from the flask and the electrode were dried under vacuum. Then, 10 mL anhydrous dichloromethane in the presence of 0.5 mL of triethylamine and 10 mg of APTE were added. The solution was stirred for 24h. The modified electrodes (APTE-Mono@GC and APTE-Multi@GC) were rinsed with dichloromethane and ultrasonicated in acetonitrile and in ultrapure water for 5 min.

2.4 Analysis

Voltammetric experiments were carried out with an Origalys OGF500 potentiostat. The working electrode (home-made GCE with 3 mm diameter), a platinum sheet counter electrode, and a saturated calomel reference electrode purchased from Origalys were used in a standard three-electrode configuration. Linear Sweep Stripping Voltammetry was performed in ultrapure water, containing 0.1 mol L^{-1} lithium perchlorate, at 0.1 V s^{-1}, under an argon

atmosphere. After optimization, the analytical protocol was performed as follows: a) Preconcentration step by complexation of cations by the APTE ligand at open circuit under stirring (500 rpm) for 5 min b) Electrodeposition of cations at -1.5 V_{SCE} for 5 min to reduce all complexed cations into their metallic form c) Linear voltammetry from -1.5 V_{SCE} to -0.4 V_{SCE} at 0.1 V s^{-1} to observe the electrochemical signal due to the oxidation of metallic compounds.

X-ray photoelectron spectroscopy (XPS) measurements were performed with an Mg Kα (hν) 1253,6 eV X-ray source using a VSW HA100 photoelectron spectrometer with a hemispherical photoelectron analyzer. The spectrometer binding energy scale was initially calibrated against the Au $4f_{7/2}$ line (84.0 eV) level.

All scans (wide spectra and resolved core level spectra) were recorded with a pass energy of 20 eV. The experimental resolution was 1.0 eV. After a Shirley background subtraction, data were treated using Spectra PRESENTS program using mixed Gaussian – Lorentzian product or sum.

Raman measurements were performed using a Renishaw inVia Reflex microspectrometer with a diode- pumped solid- state laser source excitation of 514.5 nm [48]. The laser power reaching the sample surface, through the 100X objective (numerical aperture 0.90) of a Leica DM2500 microscope, did not exceed 0.1 mW. The laser power density as well as the accumulation time and number of repetitions were varying in order to obtain relevant signal-to-noise ratios. The microspectrometer was calibrated using the 520.5 cm^{-1} line of an internal silicon standard. After Rayleigh diffusion was eliminated by edge filters, the Raman signal was first dispersed using 1,800 lines/mm signal before analysis with a deep depletion CCD detector (1,024 × 256 pixels). Renishaw Wire 4.1 software was used for instrument calibration and Raman measurements.

3. Results and discussion

3.1. Electrode functionalization

Two different paths were used to functionalize the carbon electrodes based on the electroreduction of aryldiazonium salts (Scheme 1).

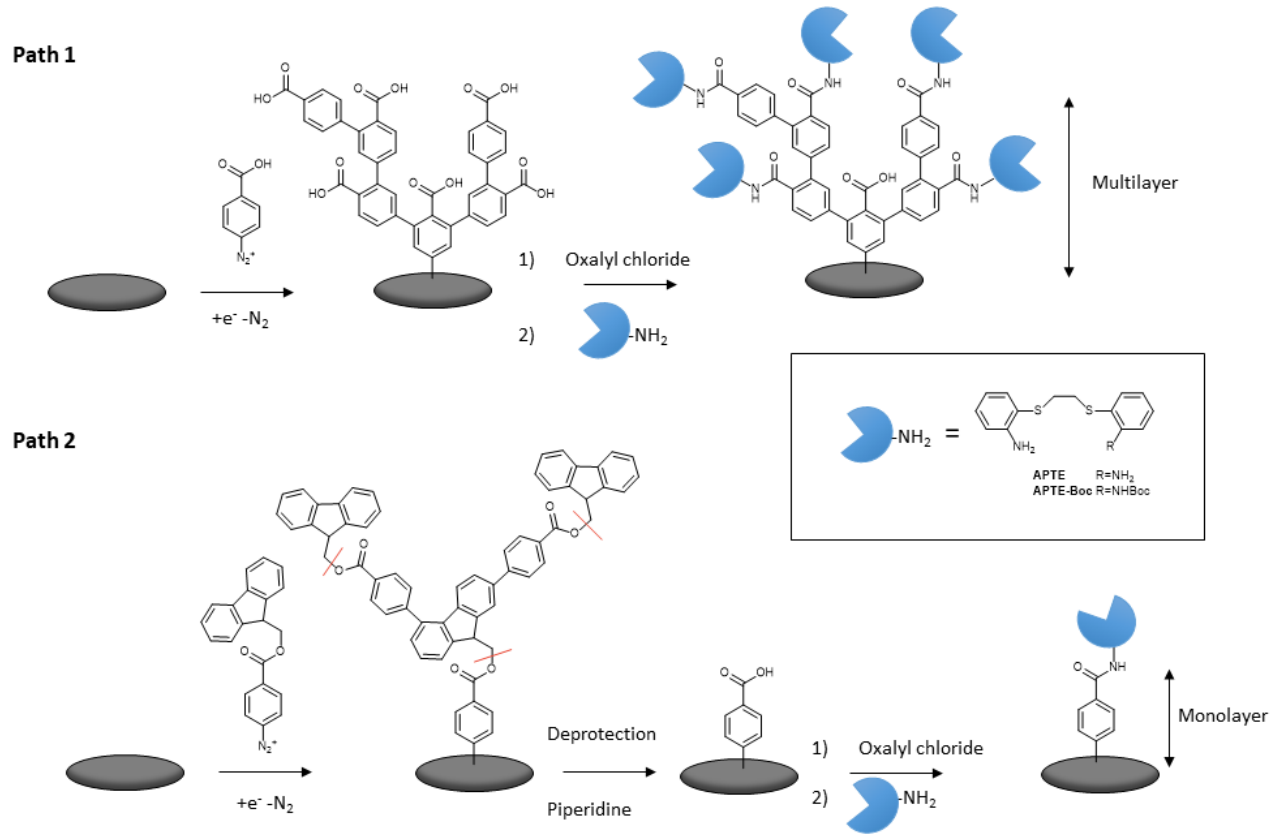

Scheme 1. The two different paths for the immobilisation of the APTE specific receptor on the electrode surfaces.

The first one (Scheme 1, Path 1) consists in a multilayer process due to the attack of aryl radicals on already grafted aromatic rings [49]. To achieve the functionalization process, the diazonium salt of 4-aminobenzoic acid was prepared *in situ* by addition at 0°C of 3 eq.

$NaNO_2$ to the amino derivative diluted in 0.5 mol L^{-1} H_2SO_4. To ensure a good reproducibility of the electrografting process, the amount of $NaNO_2$ was first optimized by ^1H NMR monitoring, to obtain the pure product (Fig. S1). The electrografting was performed by cyclic voltammetry with 5 cycles between 0 and -0.6 V_{SCE} (Fig. 1a). The decrease of the current after each cycle attested the electrode functionalization by a non-conducting layer. The efficiency of the electrografting process was also examined using dopamine as a redox probe in solution. Indeed, the electrochemical response of dopamine is known to be very sensitive to the surface state of the electrode [46]. As shown in Fig. 1c, after the electrografting process, the electrochemical signal of dopamine disappeared, due to the inhibition of electron transfer between dopamine and the electrode. The second functionalization process consists in a protection-deprotection strategy with fluorenylmethyloxy (Fm) as a COOH protecting group (Scheme 1, Path 2) [46]. It is known to form a thin functionalized organic layer on the electrode surface. Thus, the electrografting of 4-[(9-H-Fluoren-9-ylmethoxy)carbonyl]-benzene-1-diazonium salts (N_2^+-ArCOO-Fm) on carbon electrodes was performed by cyclic voltammetry with 5 scans between 0.8 and -0.7 V_{SCE} in acetonitrile. The presence of two reduction peaks has been previously ascribed to catalyzed and uncatalyzed reduction processes [50]. As for Path 1, the electrochemical current rapidly decreased (Fig. 1b), showing the efficiency of the electrografting process. The absence of dopamine signal (Fig. 1 d, red line) is also in accordance with a multilayer electrografting process with a radical attack occurring this time on the protecting Fm group. The deprotection of the carboxylic acid groups was then performed with piperidine, leading to an Ar-COOH thin organic layer on the electrode surface, as shown by the partial recovery of the dopamine electrochemical signal in Fig. 1d (green line) [46]. After the functionalization process, the APTE ligand was then covalently immobilized by a coupling reaction with accessible COOH groups. This ligand was chosen as a selective receptor of Cd^{2+} ions since it has been previously shown that its

sensitivity towards cadmium is higher than other cations such as Hg^{2+}, Cu^{2+}, Ag^{+}, Pb^{2+}, Zn^{2+}, Ni^{2+} and Co^{2+} [47].

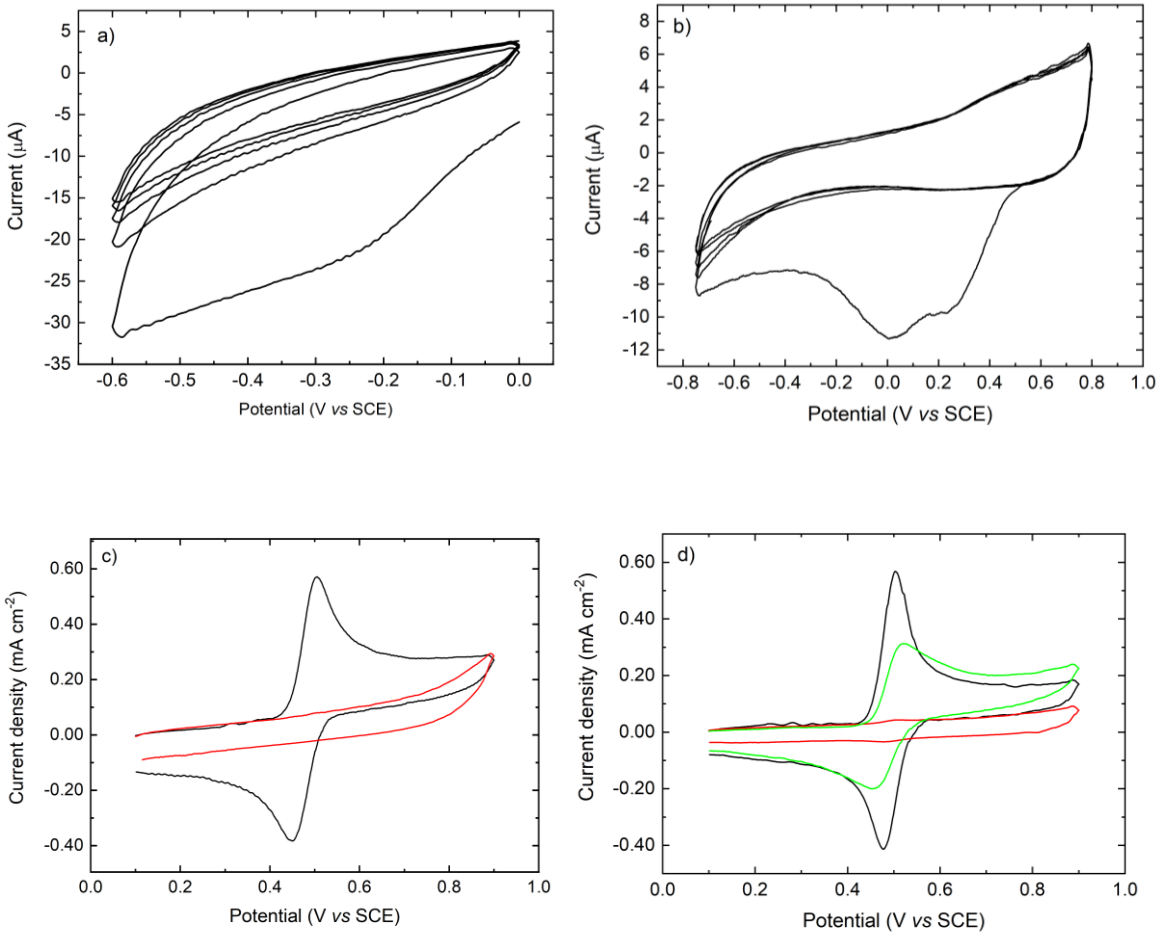

Fig. 1. Five consecutive scans at a bare GCE a) in a solution of 50 mmol L^{-1} 4-aminobenzoic acid in 0.5 mol L^{-1} H_2SO_4 (0.1 V s^{-1}) b) in a solution of 5 mmol L^{-1} N_2^{+}-ArCOO-Fm in 0.1 M $TBABF_4$-ACN (50 mV s^{-1}) and cyclic voltammograms of 5 mmol L^{-1} dopamine in 0.1 mol L^{-1} H_2SO_4 at 0.1 V s^{-1} on a bare GCE (black line) and GCE modified according to Path 1 (c) and Path 2 (d) before (red line) and after (green line) deprotection in 20% piperidine/DMF.

Whereas the reversible system of dopamine totally disappeared for the GC electrode modified according to Path 1, it was still visible after Path 2 modification. The difference of the dopamine responses on Ar-COOH GC surfaces modified according to Path 1 or 2 (Fig. 1 c

and d) suggests a higher electron barrier for electrodes modified by the multilayer process. To check if this result is effectively due to a difference in electron transfer between the two modified surfaces, kinetic studies were performed by cyclic voltammetry over a range of scan rates (v: 0.05-3 V s^{-1}) with ferrocyanide as redox probe onto the bare GC electrode and the GC electrode modified according to Path 1 and 2. Ferrocyanide (10^{-3} mol L^{-1}) has been chosen as redox probe since it is surface sensitive [51]. Figure 2 depicts the variation of peak-to-peak potential separation ΔEp with log(v) in the three systems.

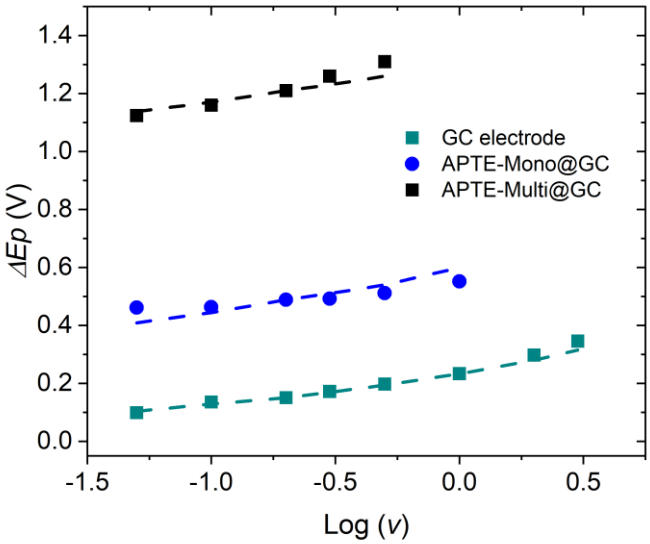

Fig. 2. Anodic and cathodic peak potential separations ΔEp as function of logarithmic scan rate v in V s^{-1} for bare and GC modified electrodes. Lines are the theoretical behaviors taking into account the ohmic drop for $k°$= 3 × 10^{-3} (green), 1 × 10^{-4} (blue), 8 × 10^{-8} (black) cm s^{-1}. Errors on the determined $k°$ are around ± 20%.

The shape of the variation of ΔEp allows the determination of the parameters $k°/D^{1/2}$ that is the ratio between the standard charge transfer rate constants $k°$ and the square root of the diffusion coefficient by simulation of the voltammograms considering the ohmic drop and capacitive current previously estimated by electrochemical impedance spectroscopy [52]. A diffusion

coefficient of 6.4×10^{-6} cm^2 s^{-1} previously determined for ferrocyanide in aqueous solution [53] was used to extract $k°$. The $k°$ value significantly decreased with the presence of an organic layer on the electrode surface, showing that the electron transfer kinetic is affected by the modification process. A value more than 1000 times lower was obtained with the multilayer process, compared with the monolayer one, highlighting the high barrier charge transfer.

The formation of bridges with the Ar-COOH GC surface by the reaction of both amino groups of APTE could prevent the complexation of Cd^{2+} ions by the receptor due to steric hindrance and to the presence of two amido groups. To prevent such immobilization process, a saturated solution of APTE was used for the coupling process, favouring the reaction of only one amino group. One amino group of APTE was also protected by a *tert*-butyloxycarbonyl (Boc) group before its immobilization on the Ar-COOH GC surface and its further deprotection (Scheme 1).

3.2. XPS analysis

The effectiveness of the functionalization processes was checked by X-ray photoelectron spectroscopy. For a better observation of the carbon peaks due to the functionalization processes, XPS was performed on gold surfaces modified according to Path 1 and 2 (Fig. 3 and Fig. S2).

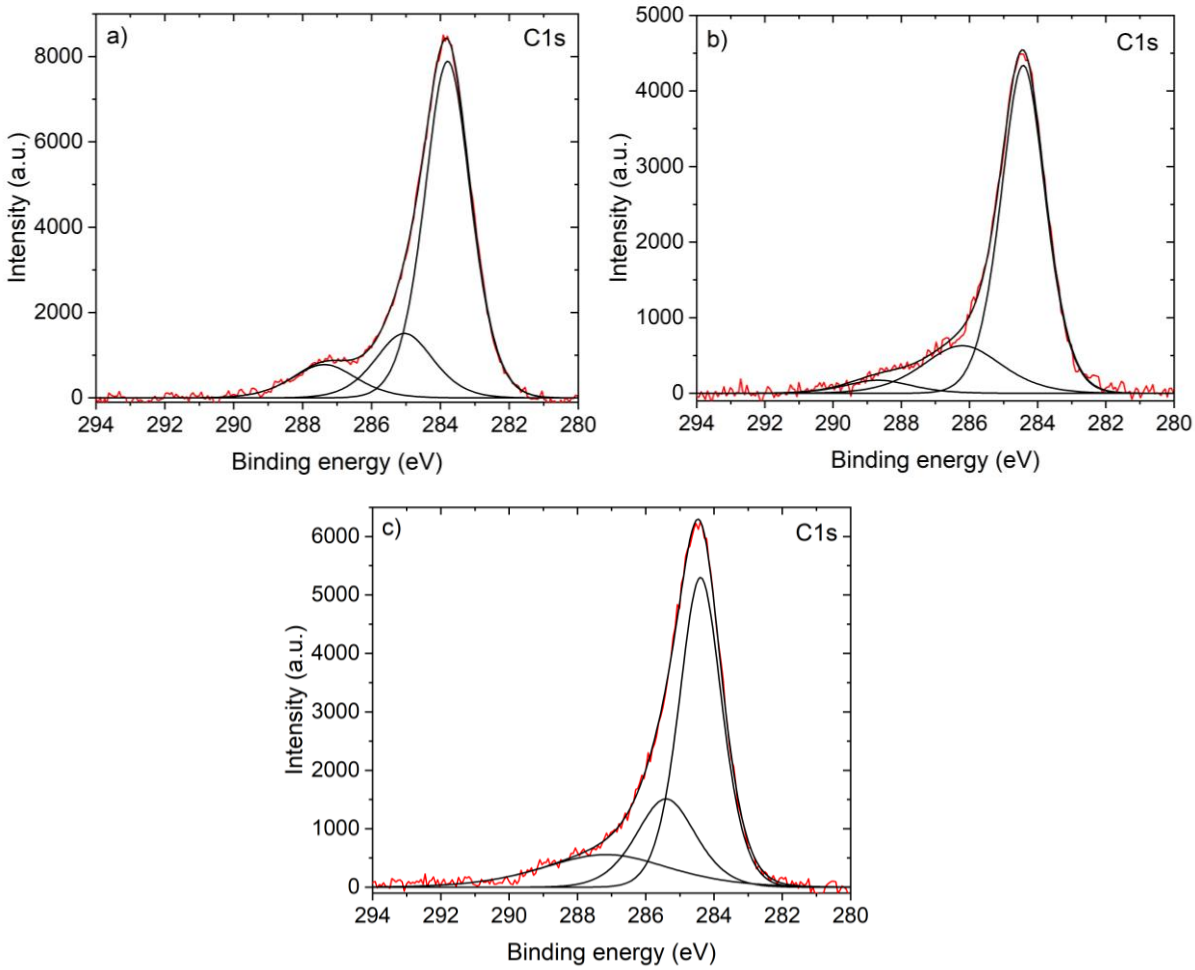

Fig. 3. XPS spectra (red) and deconvolution (black) of gold electrode modified according to Path 2 after electrografting of N_2^+-ArCOO-Fm (a), deprotection (b) and APTE coupling reaction (c).

For Path 2, before deprotection, the C1s peak was deconvoluted into three peaks at 283.8, 287.4 and 285.0 eV, assigned to C-C, -O-C=O and C-O-C(O), respectively, showing the presence of the ester group on the electrode surface. After deprotection, the peak at 286.5 eV significantly decreased (Table 1), due to the formation of a monolayer of COOH groups.

Table 1. Parameters obtained from the XPS measurements of GC electrode modified according to Path 2

Step		Binding energy (eV)	FWHM (eV) [a]	% Peak area ratio [b]
Before deprotection	$Au4f_{5/2}$	87.7	1.0	
	$Au4f_{7/2}$	84.0	1.0	
	C1s	287.4	2.3	8.5
	C1s	285.0	2.1	14.8
	C1s	283.8	1.7	61.7
	O1s	544.6	1.6	7.6
	O1s	543.1	1.6	7.3
After deprotection	$Au4f_{5/2}$	87.7	1.1	
	$Au4f_{7/2}$	84.0	1.0	
	C1s	288.7	2.4	3.9
	C1s	286.2	2.8	16.9
	C1s	284.4	1.6	65.9
	O1s	532.2	1.7	3.9
	O1s	531.1	1.9	9.3
After APTE immobilization	$Au4f_{5/2}$	87.7	1.1	
	$Au4f_{7/2}$	84.0	1.0	
	C1s	287.2	3.2	13.5
	C1s	285.4	2.6	17.2
	C1s	284.4	1.6	43.3
	O1s	531.5	2.1	16.6
	$S2p_{1/2+3/2}$	164.0	1.7	1.43
	$S2p_{3/2+3/2}$	161.9	1.7	4.3
	N1s	403	2.3	0.9
	N1s	401	2.0	0.5

[a] Full-Width Half-Maximum of peaks [b] After correction from the ionisation cross-section

The immobilization of APTE was then attested by the presence of N1s and S2p peaks (Table 1, Fig. S2). The attenuation of the double-peak occurring at 87.7 and 84.0 eV and corresponding to Au $4f_{7/2}$ and Au $4f_{5/2}$ allowed the measurement of the organic layer thickness. For a better accuracy, the thicknesses (*d*) were calculated at each step of the modification processes from the attenuation of the Au $4f_{7/2}$ peak (84.0 eV). In fact, at a given angle, the XPS intensity of gold varies according to the relation (1):

$$I(\theta) = I_{\infty} \exp\left(-\frac{d}{\lambda \cos(\theta)}\right) \quad (1)$$

Where I_{∞} is the intensity of the clean uncovered surface, d the thickness of the molecular layer on top of the surface, λ the inelastic mean free path, and θ the photoelectrons emission angle. Considering measurements at two emission angles of 0°C and 45°C, d can be deduced according to the relation 2.

$$d = \frac{ln\frac{I_{0°}}{I_{45°}}}{\left(-\frac{1}{\lambda cos0°}+\frac{1}{\lambda cos45°}\right)} \quad (2)$$

where I is the signal measured for gold surface covered by an organic layer and λ is the attenuation length of gold electrons in the organic layer (λ = 2.0 nm).

Results are given in Table 2.

Table 2. Thickness of the organic layers estimated by XPS

Functionalization	Step	Thickness (nm)
Path 1	After APTE immobilization	2.2
Path 2	Before deprotection	3
	After deprotection	0.5
	After APTE immobilization	1.3

The modification of the electrode according to Path 1 led to a thickness of 2.2 nm, as expected for a multilayer process. The thicknesses of the organic layer before and after deprotection for Path 2 (1st and 2nd steps) are in accordance with previously reported thicknesses measured by AFM scratching on PPF surfaces modified by the same method [46]. Since it is well-known that many substrates including gold and carbon can be modified by the reduction of diazonium salts [28], this result shows the good reproducibility and flexibility of the method. After immobilization of APTE, it slightly increased to 1.3 nm, about 2 times lower than for Path 1. This difference is consistent with the blocking character of the multilayer compared with the monolayer observed in the kinetic study.

3.3. Raman analysis

The gold sample modified according to Path 2 was also analyzed by Raman, since gold substrate was not Raman active (Fig. 4). The successful grafting of gold substrate was demonstrated by comparing Fig. 4a and the Raman spectrum obtained for the synthesized diazonium salt (Fig. S3). After the electrografting process, the absence of the strong peak seen

at 2293 cm^{-1} on the Raman spectra of the synthetized diazonium salt and assigned to the N≡N stretching of the N_2^+ function [54] gave the first proof of efficient grafting [55]. The two strong bands observed at 1594 and 1610 cm^{-1} (Fig. S3) and at 1600/1604 and 1610 cm^{-1}, respectively (Fig. 4) are characteristic of the fluorene group [56]. According to Chakraborty *et al.* [56], these two characteristic bands were assigned to (i) a mixture of six member ring C-C stretch and five member ring deformation mode and (ii) to aromatic C-C stretching. The medium band observed at 1585 cm^{-1} is the signature of the ortho-meta C=C stretching mode of the 1,4 benzene substituted ring [55]. After deprotection (Fig. 4b), the presence of the carboxylic acid function was attested by the symmetric C=O stretching at 1651 cm^{-1}, the O-H stretching vibration at 2936 cm^{-1} and the OH deformation vibration at 1340 cm^{-1} [57].

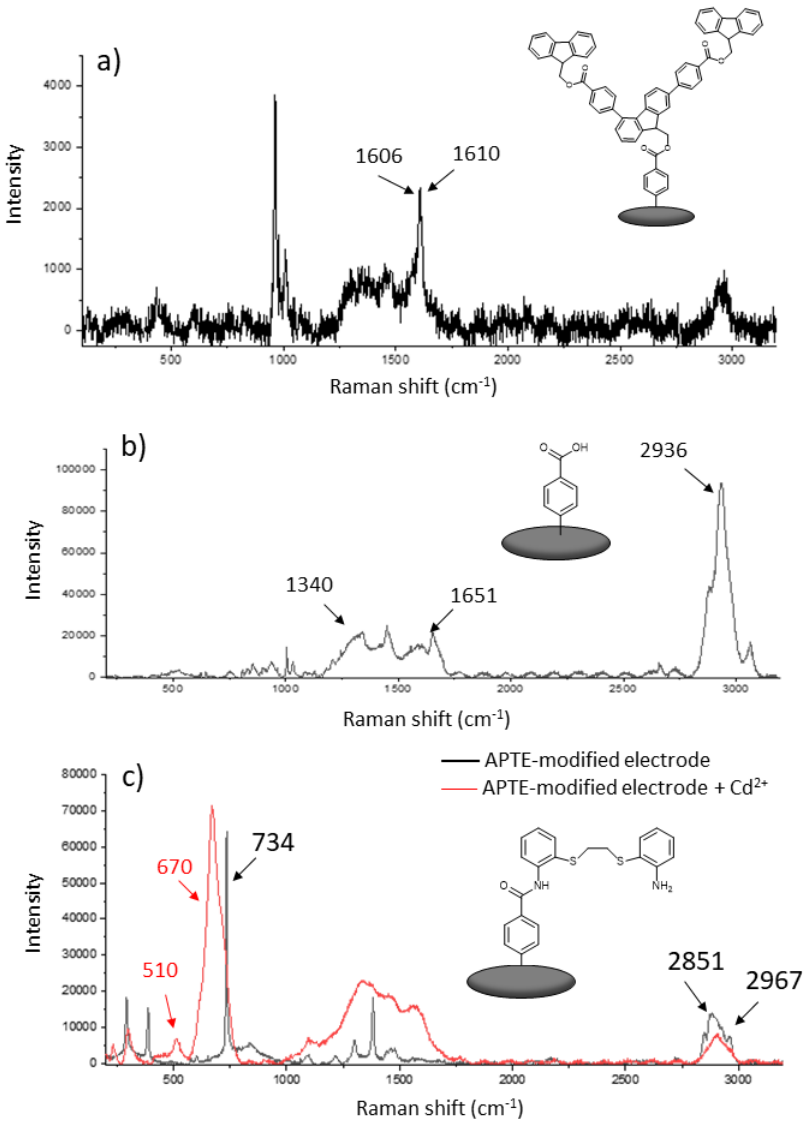

Fig. 4. Raman spectra of the electrode modified according to Path 2 after electrografting of N_2^+-ArCOO-Fm (a), deprotection (b) and APTE coupling reaction (c).

Small bands at 1593 and 1607 cm^{-1} could be due to a small amount of remaining methylfluorene protecting groups. After the coupling reaction with APTE, the peaks characteristic of the sulfur atom were found at 734, 2967 and 2851 cm^{-1}, with a small shift compared to the APTE reference (Fig. S4), due to a new environment after the covalent attachment of the molecule [57, 58].

For a better insight into the immobilized receptor ability to complex Cd^{2+}, the modified electrode was dipped in a 5×10^{-6} mol L^{-1} solution of $Cd(NO_3)_2$ for 1h and rinsed with ultrapure water. The Raman spectrum of the host-matrix interaction i.e the Cd/immobilized receptor interaction or the Cd/electrode interaction (Fig 4c) was compared to that of the $Cd(NO_3)_2$ salt (Fig. S5). The later resulted from the drying, under air atmosphere, of a drop of 10 µL of the $Cd(NO_3)_2$ solution deposited on a gold substrate. The band observed at 1048 cm^{-1} (Fig. S5), corresponding to the in-plane symmetric stretching vibrational mode of nitrate ions [59, 60] was not visible in the Raman spectrum of the Cd/electrode interaction, showing that no adsorbed or precipitated $Cd(NO_3)_2$ was present on the electrode surface.

Although cadmium is Raman inactive, its presence can be attested by the decrease of the peaks at 2851 and 2967 cm^{-1}, corresponding to the symmetric and asymmetric stretching of the S-CH_2 bounds [57]. It is also confirmed by the shift of the intense Raman peak of sulfur from 734 to 670 cm^{-1}, owing to the weakening of the C-S bound after complexation [58]. Finally, a new peak at 510 cm^{-1} could be due to the complexation of Cd^{2+} by the amino groups [57]. A distorted tetrahedral configuration complex is assumed via the interaction between the electrons of the d orbitals of Cd^{2+} and the electronic doublets of the sulfur atoms and the nitrogen ones coming from NH_2 and NH functions.

Since Raman analysis confirmed the presence of APTE on the electrode surface and the complexation of Cd^{2+}, the modified electrode was then used for Cd^{2+} detection.

4. Performance of the sensor for Cd^{2+} detection

4.1. Optimization of the analytical parameters

The APTE-modified electrodes (APTE-Multi@GC and APTE-Mono@GC for electrodes modified according to Path 1 and 2, respectively) were then used for Cd^{2+} electrochemical detection. A preconcentration step was first performed at open-circuit under stirring for the selective complexation of cadmium ions by APTE ligand onto the electrode surface. It was followed by linear sweep stripping voltammetry (LSSV) analysis without stirring to detect the complexed Cd^{2+} ions by electrochemical analysis. First attempts to preconcentrate Cd^{2+} ions (for > 5 min in 0.1 mol L^{-1} of $LiClO_4$ containing 10^{-7} mol L^{-1} of Cd^{2+} under stirring) and then dip the electrode in a solution of 0.1 mol L^{-1} $LiClO_4$ without Cd^{2+} for LSSV analysis (electrodeposition: -1.5 V_{SCE} for 5 min; stripping: 0.1 V s^{-1} between -1.5 and -0.4 V_{SCE}) did not lead to an electrochemical signal, probably due to a fast equilibrium displacement of the complexation reaction. For this reason, the analysis of Cd^{2+} was performed in the same solution in which the preconcentration step occurred to maintain Cd^{2+} ions complexed by APTE at the electrode surface. Under these investigated conditions, experimental analytical parameters were first optimized with the electrode modified according to Path 2. The preconcentration step was performed with and without stirring for 5 min. As seen in Fig. 5a, no signal was observed without stirring, highlighting its importance to improve the mass transfer of Cd^{2+} ions at the electrode for subsequent complexation with the immobilized receptor.

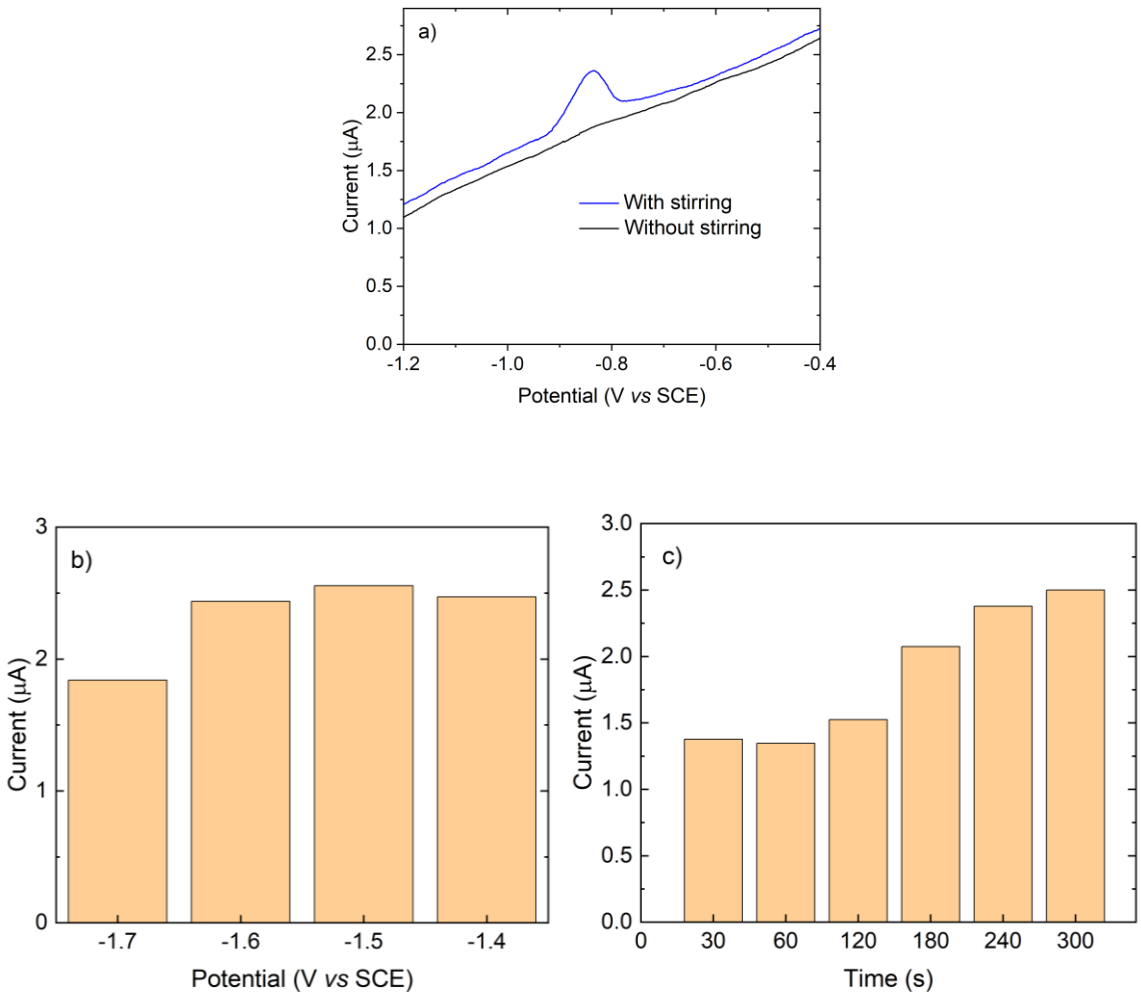

Fig. 5. a) LSSV analysis (electrodeposition: -1.5 V_{SCE} for 5 min; stripping : 0.1 V s^{-1} between -1.5 and -0.4 V_{SCE}) of a solution of 10^{-7} mol L^{-1} Cd^{2+} in 0.1 mol L^{-1} $LiClO_4$ after a 5 min preconcentration step at open circuit realized without and with stirring (500 rpm). Effect of b) the electrodeposition potential (for 5 min electrodeposition) and c) the electrodeposition time (-1.5 V_{SCE}), after a 5 min preconcentration step at open circuit under stirring (500 rpm) for a solution of 10^{-6} mol L^{-1} Cd^{2+}.

For LSSV analysis, best results were obtained with a deposition potential of -1.5 V_{SCE} (Fig. 5b). The electrochemical signal increased with the electrodeposition time for an applied potential of -1.5 V_{SCE} (Fig. 5c). A good compromise was found between the analysis time and

the electrochemical signal for an electrodeposition time of 5 min. Therefore, these optimized analytical conditions (5 min preconcentration with stirring (500 rpm) and LSSV analysis with electrodeposition at -1.5 V_{SCE} for 5 min) were used in the following experiments.

4.2 Repeatability and electrode regeneration

The repeatability of the measurements was tested in a 2×10^{-7} mol L^{-1} solution of Cd^{2+} in 0.1 mol L^{-1} $LiClO_4$ with electrodes modified according to Path 1 (multilayer) and Path 2 (monolayer). For the electrode with the multilayer, the electrochemical signal increased after each analysis, even if the final potential after the LSSV analysis was maintained at 0 V_{SCE} (Fig. 6a). A regeneration step consisting in an oxidation at 0 V_{SCE} for 10 min in 0.1 mol L^{-1} $LiClO_4$ allowed the recovery of the signal.

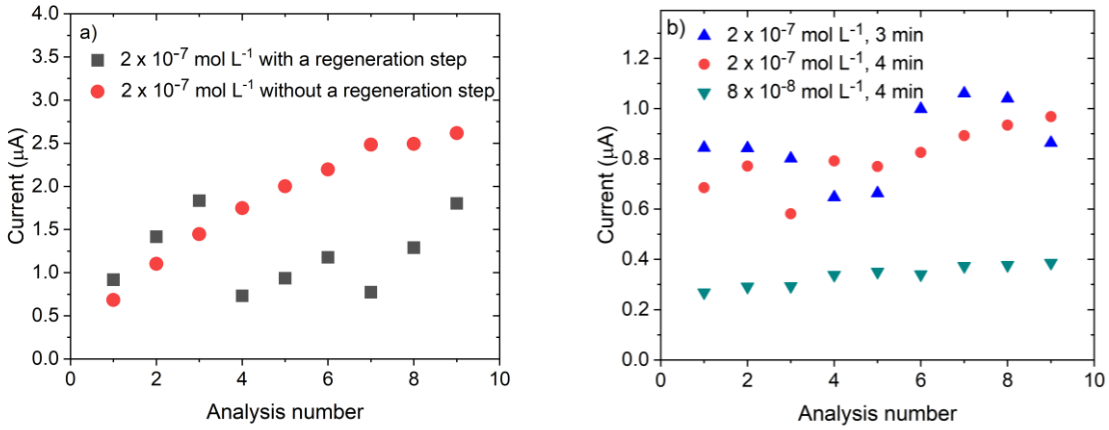

Fig. 6. Repeatability of Cd^{2+} detection in 0.1 mol L^{-1} $LiClO_4$ on GC electrode modified according to Path 1 (a) and Path 2 (b). The analysis was performed as follows: 5 min preconcentration with stirring at 500 rpm and LSSV analysis from -1.5 V_{SCE} for 5 min to 0 V_{SCE} at 0.1 V s^{-1}. For a), a regeneration step (oxidation at 0 V_{SCE} for 10 min in 0.1 mol L^{-1}

$LiClO_4$ without Cd^{2+}) was performed after 3 analyses. For b) an oxidation at 0 V_{SCE} for 3 or 4 min was performed after each analysis.

For the electrode modified with a monolayer, the increase of the electrochemical signal after each analysis was smaller and a chronoamperometry at the end of the analysis at 0 V_{SCE} was enough to obtain a repeatable signal (around ± 11%) at least for the first 5 analyses as shown in Fig. 6b for different concentrations of Cd^{2+}. It is worth noting that a regeneration consisting in a bath of 0.1 mol L^{-1} H_2SO_4 for 10 min and then a 0.5 mol L^{-1} phosphate buffer pH 7 for one night was suitable when a strong pollution of the electrode occurred.

This study clearly highlighted the poor repeatability of the analyses performed with the APTE-Mutli@GC electrode, with significant improvement with a well-controlled monolayer modification process. It is also worth noting that the covalently modified APTE-Mono@GC electrode exhibited high stability and could be used several months without degradation.

4.3. Calibration curve

The dependence of the electrochemical signal on the Cd^{2+} concentration of the analyzed solution for electrodes modified according to Path 1 and 2 is given in Fig. 7.

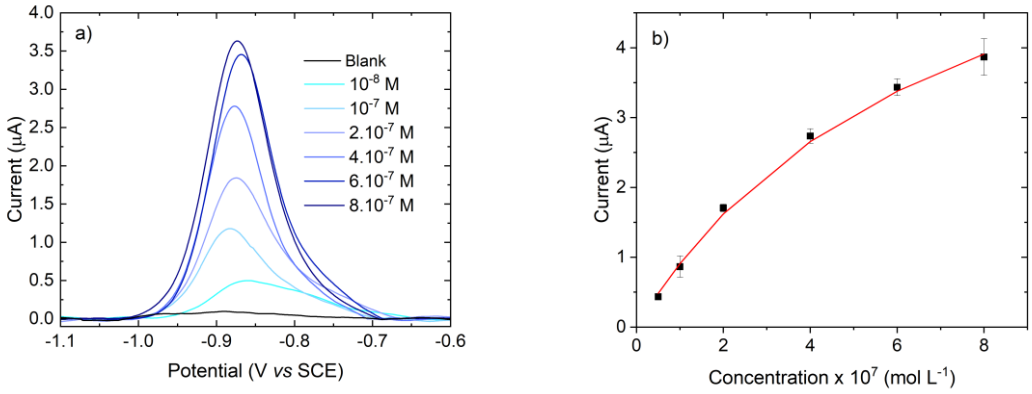

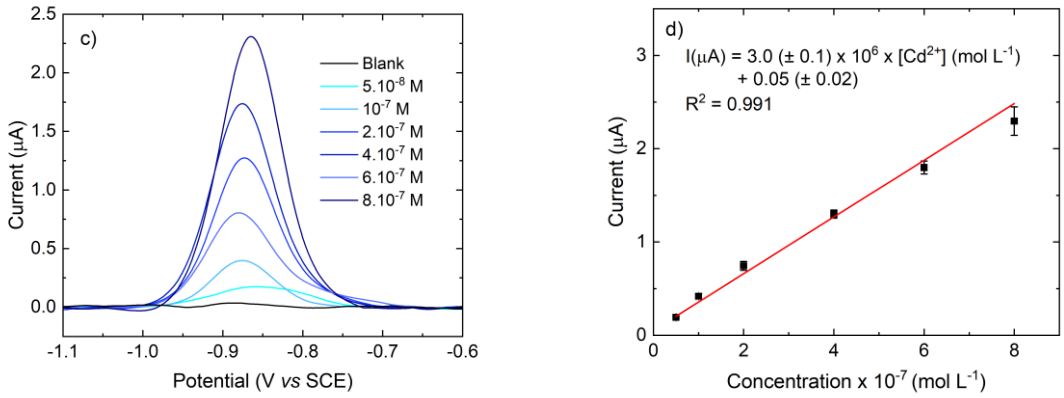

Fig. 7. Typical voltammograms obtained by LSSV analysis of trapped Cd^{2+} in a 0.1 mol L^{-1} aqueous solution of $LiClO_4$ on GC electrode modified according to Path 1 (a) and Path 2 (c) (5 min preconcentration with stirring (500 rpm) and LSSV analysis from -1.5 V_{SCE} for 5 min to -0.4 V_{SCE} at 0.1 V s^{-1}). A blank was performed under the same conditions. Electrochemical signal (maximum peak current) *versus* Cd^{2+} concentration for GC electrode modified according to Path 1 (b) and Path 2 (d). Error bars are based on two or three reproducibility measurements.

As observed in Fig. 7, the behaviour of the two modified electrodes is different. The calibration curve of the APTE-Multi@GC electrode is nonlinear in the studied concentration range (5×10^{-8} to 8×10^{-7} mol L^{-1}) (Fig. 7b). The nonlinearity of the calibration curve was expected for a sensor governed by an equilibrium process with a shape corresponding to a Langmuir-like relation (Fig. 7b, red line) [18, 19]. The calibration curve obtained for the APTE-Mono@GC electrode is almost linear. Only the last point corresponding to the highest studied concentration (8×10^{-7} mol L^{-1}) is slightly out of the correlation straight line. Higher concentrations were not tested to avoid unspecific preconcentration of uncomplexed ions onto the electrode surface. Indeed LSSV measurements on unmodified GC electrode performed in the same conditions did not give an electrochemical signal for concentrations lower than 8 ×

10^{-7} mol L^{-1}. A good correlation coefficient (> 0.99) was obtained for the APTE-Mono@GC electrode. The sensitivities measured from the slope of the linear calibration curve was 3.0 ± 0.1 × 10^{6} μA mol^{-1} L. The higher linear range observed for the APTE-Mono@GC electrode could be ascribed to lower limiting current density and affinity equilibrium constant, because of the lower amount of immobilized APTE ligand. Indeed, the higher current values obtained for the APTE-Multi@GC electrode for all studied Cd^{2+} concentrations (Fig. 7a and c) showed that a higher amount of APTE ligand covered its surface. It is interesting to note that despite the high charge transfer barrier shown by the APTE-Multi@GC electrode when redox probes such as ferrocyanide and dopamine were used, the current intensity obtained by LSSV for cadmium was high. The electron charge transfer between cadmium and the electrode seems to be less affected by the organic layer.

Interestingly, similar results were obtained for an electrode modified by the monoprotected APTE receptor (Fig. S6), suggesting that most of the APTE receptors were immobilized by only one amino group when a saturated solution of APTE was used during the coupling reaction.

The limit of detection (3 × the standard deviation of five blank determinations) was determined from equation 2 [61],

$$St\text{-}Sb \geq 3\sigma \quad (2)$$

where St is the gross analyte signal, Sb the field blank and σ the variability in the field blank. St and Sb were the maximum current intensity of the corresponding peaks [61].

A limit of detection of 3.5 × 10^{-8} mol L^{-1} (1.7 μg L^{-1}) was obtained for electrodes modified according to Path 2. It is below the European drinking water guidelines for Cd^{2+} set at 5 μg L^{-1}, underlying the interest of the method, although it could be further optimized as shown

by the classical LOD range (around 10^{-10} -10^{-9} mol L^{-1}) obtained with this type of sensor (Table S1). For the APTE-Multi@GC electrode, the linear concentration range was too small (defined with only three points) to accurately calculate the LOD. Several measurements attempted between 5×10^{-8} and 2×10^{-7} mol L^{-1} did not lead to good repeatability, making it difficult to establish a calibration line in this concentration range. A comparison was also performed with an unmodified carbon electrode. A calibration curve (Fig. S8) was drawn after optimization of the different analytical parameters (Fig. S7). No signal of Cd^{2+} was observed for concentrations $\leq 8 \times 10^{-7}$ mol L^{-1}, which is above the European drinking water guideline set as 4×10^{-8} mol L^{-1}. This result underlines all the interest in the use of such receptor to preconcentrate on the electrode surface and thus detect traces of Cd^{2+} ions.

4.4 Interfering species study

The selectivity of the modified electrodes for Cd^{2+} was examined in the presence of common metal ion interferents: Cu^{2+}, Pb^{2+}, Hg^{2+}, Zn^{2+}, Co^{2+}, Cr^{2+}, Mn^{2+} and Fe^{3+}. The analysis of Cd^{2+} (2×10^{-7} mol L^{-1}) was performed on a modified electrode and then the interferent ion was added at the same concentration (2×10^{-7} mol L^{-1}) in the solution for comparison. Similar experiments were performed with an unmodified electrode with higher concentrations of 10^{-6} mol L^{-1}. As shown in Fig. 8, Cd^{2+} interfered with all studied ions when an unmodified carbon electrode was used. A significant improvement in selectivity is observed with the modified electrodes for all studied ions. For Cu^{2+}, Pb^{2+}, Zn^{2+}, Co^{2+} and Mn^{2+} ions a higher electrochemical signal was obtained with the APTE-Multi@GC electrode compared with the APTE-Mono@GC one. Since at 2×10^{-7} mol L^{-1} no signal can be observed without the preconcentration step, this effect could be due to the higher number of receptors on the electrode surface, preventing unspecific preconcentration to occur.

The same experiment was performed with the Mono@GC electrode modified by Boc-APTE with two interferent ions: Pb^{2+} and Co^{2+}. The electrochemical signal of Cd^{2+} decreased by around 40% and 60% for Pb^{2+} and Co^{2+}, respectively, which is consistent with results obtained with the APTE-Mono@GC electrode (Fig. 8). These experiments confirm that the formation of bridges with the COOH-functionalized surface was limited when a saturated solution of APTE was used during its covalent immobilization.

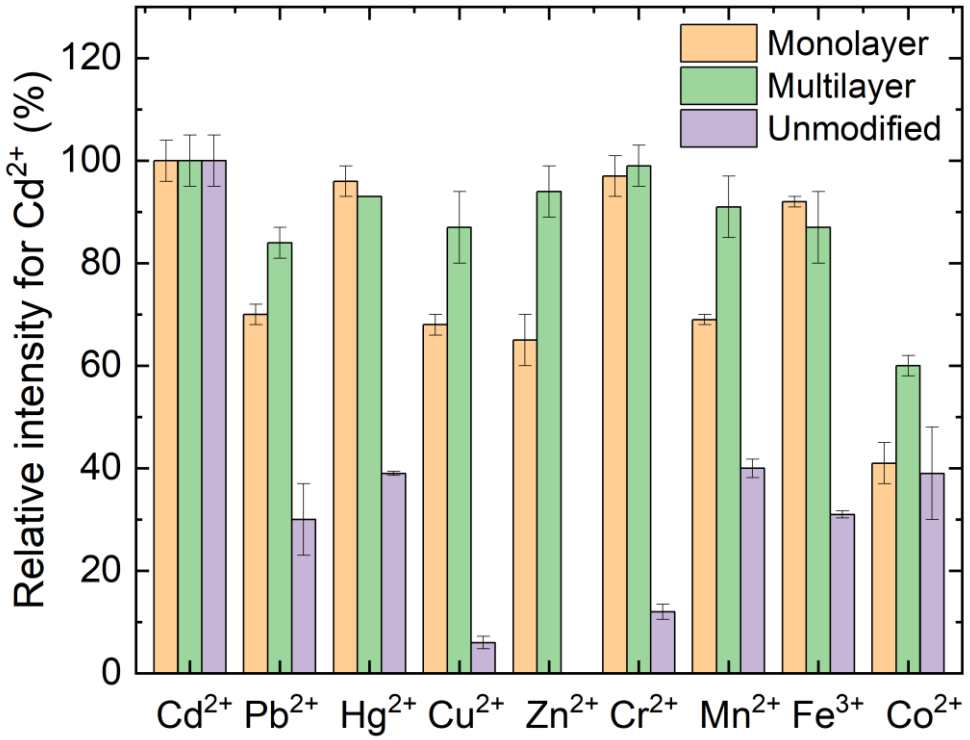

Fig. 8. Relative intensity for Cd^{2+} (initial concentration: 2 10^{-7} mol L^{-1} and 10^{-6} mol L^{-1} for modified and unmodified electrodes, respectively) alone (first column) or with the same concentration of interferent ion. No signal was observed in the presence of Zn^{2+} for the unmodified electrode. Error bars are based on two measurements.

5. Conclusions

In this study, we prepared a simple and robust electrochemical sensor for specific cadmium detection through the covalent immobilization of a well-known cadmium complexing agent on carbon electrode. Beyond the preparation of an efficient, mercury-free and easily regenerable sensor, this work highlights the advantages of using a well-controlled monolayer electrografting method compared with a multilayer one to prepare ligand-modified sensor. APTE-modified electrodes were prepared by two fast and simple electrografting methods, leading either to a multilayer or to a monolayer of immobilized linkers. XPS and Raman spectroscopy clearly demonstrated (i) the successful functionalization of carbon electrodes by a multilayer or a monolayer of benzoic acid groups, (ii) subsequent immobilization of the specific APTE receptor and (iii) Cd^{2+}/APTE interaction. The performance and robustness of APTE-modified electrodes for Cd^{2+} detection was investigated and compared with an unmodified electrode. Several conclusions can be drawn from this study. First, APTE-Mono@GC electrode led to better repeatability than its multilayer analogue. It exhibited high stability due to the covalent immobilization of the APTE ligand and could be easily regenerated by a short oxidation step at the end of each analysis sequence, while APTE-Multi@GC electrode required a frequent washing step, increasing significantly the analysis time. Second, APTE-Mono@GC electrode exhibited a good linear concentration range from 5×10^{-8} to 8×10^{-7} mol L^{-1}, while APTE-Multi@GC electrode gave a calibration curve with a shape corresponding to a Langmuir-like relation. Third, the interest of the selective preconcentration step was clearly highlighted. APTE-Mono@GC electrode had a LOD of 1.7 μg L^{-1}, lower than the European drinking water guidelines (5 μg L^{-1}), while no electrochemical response was observed with the unmodified electrode for Cd^{2+} concentration lower than 8×10^{-7} mol L^{-1}. Both modified electrodes showed better selectivity than the

unmodified one. Further work is in progress to optimize the sensor operating conditions such as the electrolytic medium, the analytical conditions, and check the matrix effect and real samples. Finally, this work highlights the importance of the method used to functionalize the electrode surface for sensing application. A stable and well-controlled electrografting process leading to a monolayer organic film appears as a method of choice to prepare sensors with selective receptors. Its application to other sensors requiring a selective preconcentration step would be interesting to investigate.

Acknowledgements

This work was supported by the French National Agency (ANR-18-CE42-0011, Programme AAPG 2018). We thank the Origalys company for lending us impedance analysis.

References

[1] L. Friberg, Cadmium and the kidney., Environ. Health Perspect., 54 (1984) 1-11.

[2] J.O. Nriagu, J.M. Pacyna, Quantitative assessment of worldwide contamination of air, water and soils by trace metals, Nature, 333 (1988) 134-139.

[3] B. Salbu, E. Steinnes, Trace Elements in Natural Water, CRC Press, London, 1996.

[4] A.M. Ure, C.M. Davidson, Editors, Chemical Speciation in the Environment, Blackie Academic and Professional, Chapman and Hall, London, 1995.

[5] A. Picot, Le trio mercure, plomb, cadmium, http://wwwhyperactifnet/images/Picot_le_trio_des_toxiquespdf.

[6] M. Miquel, Les effets des métaux lourds sur l'environnement et la santé. Rapport d'informations. , Office Parlementaire d'Evaluation des Choix Scientifiques et Technologiques, Assemblée Nationale-Sénat, 2001.

[7] Order 2001-1220, 20 december 2001 and European communities regulation 2007, S.I. n°278 of 2007.

[8] D.C. Baxter, W. Frech, Speciation of lead in environmental and biological samples, Pure & Appl. Chem., 67 (1995) 615-648.

[9] R.E. Farrell, J.J. Germida, P.M. Huang, Biotoxicity of Mercury as Influenced by Mercury(II) Speciation, Appl. Environ. Microbiol., 56 (1990) 3006-3016.

[10] W.G. Sunda, D.W. Engel, R.M. Thuotte, Effect of chemical speciation on toxicity of cadmium to grass shrimp, Palaemonetes pugio: Importance of free cadmium ion, Environ. Sci. Technol., 12 (1978) 409-413.

[11] M. Jin, H. Yuan, B. Liu, J. Peng, L. Xu, D. Yang, Review of the distribution and detection methods of heavy metals in the environment, Anal. Methods, 12 (2020) 5747-5766.

[12] C. Parat, L. Authier, S. Betelu, N. Petrucciani, M. Potin-Gautier, Determination of labile cadmium using a screen-printed electrode modified by a microwell, Electroanalysis, 19 (2007) 403-406.

[13] A.J. Bard, L.R. Faulkner, Electrochemical Methods: Fundamentals and Applications, 2nd Ed., John Wiley & Sons, New York, 2001.

[14] A. Shaban, L. Eddaif, T. Szabó, A Mini-review on the Application of Chemically Modified Sensing Platforms for the Detection of Heavy Metal Ions in Water, Curr. Anal. Chem., 19 (2023) 199-219.

[15] D.W. Arrigan, Tutorial review. Voltammetric determination of trace metals and organics after accumulation at modified electrodes, Analyst, 119 (1994) 1953-1966.

[16] G. March, T.D. Nguyen, B. Piro, Modified electrodes used for electrochemical detection of metal ions in environmental analysis, Biosensors, 5 (2015) 241-275.

[17] L. Pujol, D. Evrard, K. Groenen-Serrano, M. Freyssinier, A. Ruffien-Cizsak, P. Gros, Electrochemical sensors and devices for heavy metals assay in water: the French groups' contribution, Front. Chem., 2 (2014) 19.

[18] R. Nasraoui, D. Floner, F. Geneste, Analytical performances of a flow electrochemical sensor for preconcentration and stripping voltammetry of metal ions, J. Electroanal. Chem., 629 (2009) 30-34.

[19] R. Nasraoui, D. Floner, C. Paul-Roth, F. Geneste, Flow electroanalytical system based on cyclam-modified graphite felt electrodes for lead detection, J. Electroanal. Chem., 638 (2010) 9-14.

[20] S. Betelu, C. Parat, N. Petrucciani, A. Castetbon, L. Authier, M. Potin-Gautier, Semicontinuous monitoring of cadmium and lead with a screen-printed sensor modified by a membrane, Electroanalysis, 19 (2007) 399-402.

[21] S. Betelu, C. Vautrin-Ul, A. Chausse, Novel 4-carboxyphenyl-grafted screen-printed electrode for trace Cu(II) determination, Electrochem. Commun., 11 (2009) 383-386.

[22] T. kokab, A. Shah, J. Nisar, A.M. Khan, S.B. Khan, A.H. Shah, Tripeptide Derivative-Modified Glassy Carbon Electrode: A Novel Electrochemical Sensor for Sensitive and Selective Detection of Cd^{2+} Ions, ACS Omega, 5 (2020) 10123-10132.

[23] T. Kokab, A. Shah, F.J. Iftikhar, J. Nisar, M.S. Akhter, S.B. Khan, Amino Acid-Fabricated Glassy Carbon Electrode for Efficient Simultaneous Sensing of Zinc(II), Cadmium(II), Copper(II), and Mercury(II) Ions, ACS Omega, 4 (2019) 22057-22068.

[24] F.-F. Wang, C. Liu, J. Yang, H.-L. Xu, W.-Y. Pei, J.-F. Ma, A Sulfur-Containing Capsule-Based Metal-Organic electrochemical sensor for Super-Sensitive capture and detection of multiple Heavy-Metal ions, Chem. Eng. J., 438 (2022) 135639.

[25] P. Allongue, M. Delamar, B. Desbat, O. Fagebaume, R. Hitmi, J. Pinson, J.-M. Saveant, Covalent Modification of Carbon Surfaces by Aryl Radicals Generated from the Electrochemical Reduction of Diazonium Salts, J. Am. Chem. Soc., 119 (1997) 201-207.

[26] M. Delamar, R. Hitmi, J. Pinson, J.M. Saveant, Covalent modification of carbon surfaces by grafting of functionalized aryl radicals produced from electrochemical reduction of diazonium salts, J. Am. Chem. Soc., 114 (1992) 5883-5884.

[27] D. Hetemi, V. Noel, J. Pinson, Grafting of diazonium salts on surfaces: application to biosensors, Biosensors, 10 (2020) 4.

[28] J.J. Gooding, Advances in interfacial design for electrochemical biosensors and sensors: aryl diazonium salts for modifying carbon and metal electrodes, Electroanalysis, 20 (2008) 573-582.

[29] I. Bakas, Z. Salmi, S. Gam-Derouich, M. Jouini, S. Lepinay, B. Carbonnier, A. Khlifi, R. Kalfat, F. Geneste, Y. Yagci, M.M. Chehimi, Molecularly imprinted polymeric sensings layers grafted from aryl diazonium-modified surfaces for electroanalytical applications. A mini review, Surf. Interface Anal., 46 (2014) 1014-1020.

[30] C. Cao, Y. Zhang, C. Jiang, M. Qi, G. Liu, Advances on Aryldiazonium Salt Chemistry Based Interfacial Fabrication for Sensing Applications, ACS Appl. Mater. Interfaces, 9 (2017) 5031-5049.

[31] J.J. Gooding, G. Liu, A.L. Gui, The use of aryl diazonium salts in the fabrication of biosensors and chemical sensors, in: M.M. Chehimi (Ed.), Wiley-VCH, Wiley, Weinheim, Germany, 2012, pp. 197-218.

[32] J.J. Gooding, S. Ciampi, The molecular level modification of surfaces: From self-assembled monolayers to complex molecular assemblies, Chem. Soc. Rev., 40 (2011) 2704-2718.

[33] D. Belanger, J. Pinson, Electrografting: a powerful method for surface modification, Chem. Soc. Rev., 40 (2011) 3995-4048.

[34] B. Feier, D. Floner, C. Cristea, R. Sandulescu, F. Geneste, Development of a novel flow sensor for copper trace analysis by electrochemical reduction of 4-methoxybenzene diazonium salt, Electrochem. Commun., 31 (2013) 13-15.

[35] C. Jiang, S. Moraes Silva, S. Fan, Y. Wu, M.T. Alam, G. Liu, J. Justin Gooding, Aryldiazonium salt derived mixed organic layers: from surface chemistry to their applications, J. Electroanal. Chem., 785 (2017) 265-278.

[36] G. Liu, J. Liu, T. Boecking, P.K. Eggers, J.J. Gooding, The modification of glassy carbon and gold electrodes with aryl diazonium salt: The impact of the electrode materials on the rate of heterogeneous electron transfer, Chem. Phys., 319 (2005) 136-146.

[37] J.C. Harper, R. Polsky, S.M. Dirk, D.R. Wheeler, S.M. Brozik, Electroaddressable selective functionalization of electrode arrays: catalytic NADH detection using aryl diazonium modified gold electrodes, Electroanalysis, 19 (2007) 1268-1274.

[38] Y.R. Leroux, H. Fei, J.-M. Noel, C. Roux, P. Hapiot, Efficient Covalent Modification of a Carbon Surface: Use of a Silyl Protecting Group To Form an Active Monolayer, J. Am. Chem. Soc., 132 (2010) 14039-14041.

[39] C. Combellas, F. Kanoufi, J. Pinson, F.I. Podvorica, Sterically Hindered Diazonium Salts for the Grafting of a Monolayer on Metals, J. Am. Chem. Soc., 130 (2008) 8576-8577.

[40] D. Hetemi, F. Kanoufi, C. Combellas, J. Pinson, F.I. Podvorica, Electrografting of Alkyl Films at Low Driving Force by Diverting the Reactivity of Aryl Radicals Derived from Diazonium Salts, Langmuir, 30 (2014) 13907-13913.

[41] T. Menanteau, E. Levillain, T. Breton, Electrografting via Diazonium Chemistry: From Multilayer to Monolayer Using Radical Scavenger, Chem. Mater., 25 (2013) 2905-2909.

[42] L. Santos, A. Mattiuzzi, I. Jabin, N. Vandencasteele, F. Reniers, O. Reinaud, P. Hapiot, S. Lhenry, Y. Leroux, C. Lagrost, One-Pot Electrografting of Mixed Monolayers with Controlled Composition, J. Phys. Chem. C, 118 (2014) 15919-15928.

[43] L.T. Nielsen, K.H. Vase, M. Dong, F. Besenbacher, S.U. Pedersen, K. Daasbjerg, Electrochemical Approach for Constructing a Monolayer of Thiophenolates from Grafted Multilayers of Diaryl Disulfides, J. Am. Chem. Soc., 129 (2007) 1888-1889.

[44] I. Lopez, S. Dabos-Seignon, T. Breton, Use of Selective Redox Cross-Inhibitors for the Control of Organic Layer Formation Obtained via Diazonium Salt Reduction, Langmuir, 35 (2019) 11048-11055.

[45] Y.R. Leroux, F. Hui, P. Hapiot, A protecting-deprotecting strategy for structuring robust functional films using aryldiazonium electroreduction, J. Electroanal. Chem., 688 (2013) 298-303.

[46] L. Lee, H. Ma, P.A. Brooksby, S.A. Brown, Y.R. Leroux, P. Hapiot, A.J. Downard, Covalently anchored carboxyphenyl monolayer via aryldiazonium ion grafting: a well-defined reactive tether layer for on-surface chemistry, Langmuir, 30 (2014) 7104-7111.

[47] S. Ramezani, M. Ghobadi, B.N. Bideh, Voltammetric monitoring of Cd(II) by nano-TiO2 modified carbon paste electrode sensitized using 1,2-bis-[o-aminophenylthio]ethane as a new ion receptor, Sens. Actuators, B, 192 (2014) 648-657.

[48] N. Saspiturry, A. Lahfid, T. Baudin, L. Guillou-Frottier, P. Razin, B. Issautier, B. Le Bayon, O. Serrano, Y. Lagabrielle, B. Corre, Paleogeothermal Gradients Across an Inverted Hyperextended Rift System: Example of the Mauléon Fossil Rift (Western Pyrenees), Tectonics, 39 (2020) e2020TC006206.

[49] J. Pinson, F. Podvorica, Attachment of organic layers to conductive or semiconductive surfaces by reduction of diazonium salts, Chem. Soc. Rev., 34 (2005) 429-439.

[50] L. Lee, P.A. Brooksby, P. Hapiot, A.J. Downard, Electrografting of 4-Nitrobenzenediazonium Ion at Carbon Electrodes: Catalyzed and Uncatalyzed Reduction Processes, Langmuir, 32 (2016) 468-476.

[51] K.E. Berg, Y.R. Leroux, P. Hapiot, C.S. Henry, SECM Investigation of Carbon Composite Thermoplastic Electrodes, Anal. Chem., 93 (2021) 1304-1309.

[52] M. Li, S. Liu, L. Xie, J. Yan, C. Lagrost, S. Wang, G. Feng, P. Hapiot, B. Mao, Charge Transfer Kinetics at Ag(111) Single Crystal Electrode/Ionic Liquid Interfaces: Dependence on the Cation Alkyl Side Chain Length, ChemElectroChem, 8 (2021) 983-990.

[53] J. Moldenhauer, M. Meier, D.W. Paul, Rapid and Direct Determination of Diffusion Coefficients Using Microelectrode Arrays, J. Electrochem. Soc., 163 (2016) H672-H678.

[54] S. Betelu, I. Tijunelyte, L. Boubekeur-Lecaque, I. Ignatiadis, A.C. Schnepf, E. Guenin, N. Bouchemal, N. Felidj, E. Rinnert, M. Lamy de la Chapelle, Raman Characterization of Phenyl-Derivatives: From Primary Amine to Diazonium Salts, , J. Org. Inorg. Chem., 3 (2017) 1.

[55] S. Betelu, I. Tijunelyte, L. Boubekeur-Lecaque, I. Ignatiadis, J. Ibrahim, S. Gaboreau, C. Berho, T. Toury, E. Guenin, N. Lidgi-Guigui, N. Felidj, E. Rinnert, M.L.d.l. Chapelle, Evidence of the Grafting Mechanisms of Diazonium Salts on Gold Nanostructures, J. Phys. Chem. C, 120 (2016) 18158-18166.

[56] S. Chakraborty, P. Das, S. Manogaran, P.K. Das, Vibrational spectra of fluorene, 1-methylfluorene and 1,8-dimethylfluorene, Vib. Spectrosc., 68 (2013) 162-169.

[57] G. Socrates, Infrared and Raman Characteristic Group Frequencies: Tables and Charts, 3rd Edition, 2004.

[58] B.J. Palys, D.M.W. van den Ham, W. Briels, D. Feil, Resonance Raman spectra of phthalocyanine monolayers on different supports. A normal mode analysis of zinc phthalocyanine by means of the MNDO method, J. Raman Spectrosc., 26 (1995) 63-76.

[59] Y.J. Liu, T. Zhu, D.F. Zhao, Z.F. Zhang, Investigation of the hygroscopic properties of $Ca(NO_3)_2$ and internally mixed $Ca(NO_3)_2/CaCO_3$ particles by micro-Raman spectrometry, Atmos. Chem. Phys., 8 (2008) 7205-7215.

[60] B.J. Krueger, V.H. Grassian, J.P. Cowin, A. Laskin, Heterogeneous chemistry of individual mineral dust particles from different dust source regions: the importance of particle mineralogy, Atmos. Environ., 38 (2004) 6253-6261.

[61] D. MacDougall, W.B. Crummett, et al., Guidelines for data acquisition and data quality evaluation in environmental chemistry, Anal. Chem., 52 (1980) 2242-2249.